ACS APPLIED MATERIALS & INTERFACES

Research Article

www.acsami.org

Polyion Multilayers with Precise Surface Charge Control for Antifouling

Xiaoying Zhu,[†] Dominik Jańczewski,*[,†,⊥] Shifeng Guo,[†] Serina Siew Chen Lee,[‡] Fernando Jose Parra Velandia,[‡] Serena Lay-Ming Teo,[‡] Tao He,[†] Sreenivasa Reddy Puniredd,[†] and G. Julius Vancso*[,§,∥]

[†]Institute of Materials Research and Engineering, A*STAR (Agency for Science, Technology, and Research), 3 Research Link, Singapore 117602

[‡]Tropical Marine Science Institute, National University of Singapore, 18 Kent Ridge Road, Singapore 119227

[§]Institute of Chemical and Engineering Sciences, A*STAR, 1, Pesek Road, Jurong Island, Singapore 627833

[∥]MESA+ Institute for Nanotechnology, Materials Science and Technology of Polymers, University of Twente, P.O. Box 217, 7500 AE Enschede, The Netherlands

Supporting Information

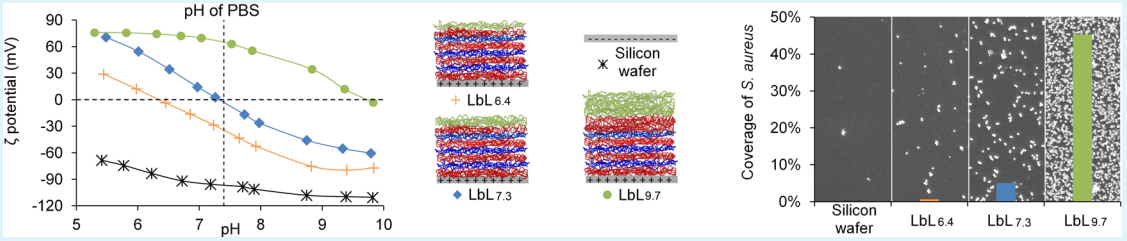

ABSTRACT: We report on a molecular fabrication approach to precisely control surface ζ potentials of polymeric thin layers constructed by electrostatic layer-by-layer (LbL) assembly methods. The protocol established allows us to achieve surface isoelectric points (IEP) in the pH range of 6−10. Poly(acrylic acid) (PAA, a weak polyanion) and poly(diallyldimethylammonium chloride) (PDADMAC, a strong polycation) were chosen to build up the bulk films. The weak polycation polyethylenimine (PEI) was applied as a top layer. A unique feature of this approach is that the chemical composition of the top layer is not affected by the manipulation of the ζ potential of the films. Surface charge tuning is achieved by controlling the degree of ionization of the weak polyelectrolytes at various pH values and subsequent manipulation of the amount of polyelectrolyte deposited in the penultimate and last layers, respectively. Following assembly and characterization, the films were used as candidates for antifouling surfaces. The fouling behavior of barnacle cyprids and bacteria on the LbL films with similar hydrophilicity and roughness but different surface charge densities were studied. We found that more cyprids of *Amphibalanus amphitrite* settled on the negatively charged LbL film compared to the neutral or positively charged LbL film. In bacterial adhesion tests employing *Pseudomonas*, *Escherichia coli*, and *Staphylococcus aureus*, more bacteria were observed on the positively charged LbL film compared with the neutral and negatively charged LbL films, possibly as a result of the negative potential of the bacterial cell wall. The procedures proposed allow one to adjust surface isoelectric points of LbL architectures to achieve optimal antifouling performance of a given material taking into account specific pH values of the environment and the character of the fouler.

KEYWORDS: *surface charge tuning, polyelectrolyte, layer-by-layer assembly, composite multilayers, antifouling*

1. INTRODUCTION

Biofouling is the accumulation of biological matter and growth of microorganisms, plants, or animals on surfaces.[1] The phenomenon may occur on any surface immersed in an aquatic environment, in any biological ecosystem, and, in the case of synthetic surfaces, it is frequently associated with economic and healthcare consequences. Fouling is recognized as a problem for biomedical applications,[2] water treatment processes,[3] and in the maritime industries.[4] Protein adsorption on biomedical implants may not only diminish the performance of the devices[5] but can also cause harmful side effects, such as thrombosis.[6] A conditioning layer formed by adsorbed proteins on the implanted devices may boost the colonization of microorganisms, resulting in inflammation.[1] The attachment of bacteria and subsequent formation of biofilm results in contamination and increased risk of infection.[1,2] Membrane fouling caused by biological substances block the membrane pores, increasing the operational pressure and decreasing the

Received: October 24, 2014
Accepted: December 8, 2014
Published: December 8, 2014

permeate flux in filtration systems. Membrane biofouling is usually permanent and irreversible, resulting in the need for more frequent replacement of the membrane, which significantly contributes to the application cost.[3] Marine biofouling[4,7,8] affects structures critical to the maritime industry such as ship surfaces, harbor installations, oil rigs, underwater sensors, and pipelines.[9] In summary, biofouling is a central problem that needs enhanced understanding and control.

Various strategies have been proposed to combat biofouling. The most widely employed methods deter or kill fouling organisms using bioactive substances.[7] Unfortunately, biocides are frequently toxic not only to the target microorganisms but also to other species[4] or cells in the vicinity.[1] Moreover, many biocides are poorly degradable and result in permanent pollution of the environment.

An environmentally friendly alternative in fouling management can be achieved using materials exhibiting low adhesion, thus preventing the attachment of foulants. This strategy can be implemented by engineering the interactions between the adhering objects and protected surface at different stages of the foulant attachment process. Importantly, employing low adhesion strategies is useful not only deterring organism attachment but also to prevent the adhesion of biomacromolecules such as proteins. Nonadhesive materials can be fabricated by tuning the surface properties,[1,10] including control of microtopography (or morphology),[11] roughness,[12] surface free energy (or wettability),[13,14] and surface charge.[15,16] Because most of the foulants (such as bacteria and proteins) are charged entities, electrostatic interaction plays an important role in bioadhesion, particularly during the initial stages of fouling.[17,18] Screening of the electrostatic interactions is usually listed as a prerequisite for preparing low-fouling materials.[19] Numerous studies that discuss the influence of surface charge on fouling properties consider the electrostatic potential as a parameter associated with the chemical constituents present at the surface without a direct consideration of the actual zeta potential (hereinafter named ζ potential). It is known that values of the isoelectric point (IEP) of a surface are dependent on many factors, in particular on the quantity and strength of the respective acid and base components of the grafted groups.[20] As a result, the surface is charge neutral only at a specific pH which is frequently not equal to the pH of the environment investigated in the fouling experiments.

Several methods have been reported to control and adjust the effective net charge of a surface. Treatment under ambient conditions with high energy irradiation,[21] or by strong oxidants[22] renders surfaces to become covered with ionic functional groups. Because the charging mechanism in these cases is usually related to radical oxidation, the resulting values of the ζ potential become negative, making fine-tuning of charge difficult. In another approach, alkanethiolates terminated with positively or negatively charged functional groups were combined to prepare self-assembled monolayers (SAMs) with different character.[16,19,23] Such surface charge tuned SAMs have also been used to study whether barnacle cyprids of *Amphibalanus amphitrite* prefer specific surface charges. These studies revealed that more cyprids settled on the negatively charged SAMs than on the neutral and positively charged SAMs.[16] The mixing of different chemical entities on the substrate (e.g., bases and acids) is a disadvantage for this approach because electrostatic contributions to surface interactions are hard to isolate from other chemically induced effects (e.g., hydrogen bonding, van der Waals interactions, or hydrophobicity).

Polymers were broadly used to control electrostatic charge distributions. For example, the charge of polymer brushes can be adjusted by polymerizing mixtures of cationic and anionic monomers.[18,24,25] Such oppositely charged monomers in different ratios were used to grow polymer brushes from polypropylene surface to prepare grafts with and without net charge.[18] A variety of positively and negatively charged molecules have also been introduced into polymeric matrices to prepare charged hydrogels for control of protein adsorption.[26]

Electrostatic layer-by-layer (LbL) assembly is a convenient, cheap and fast method to prepare polymeric films[27−30] or microcapsules.[31,32] It can be carried out by alternatively dipping of substrates in oppositely charged polyelectrolyte solutions or by spraying these solutions onto a surface.[33] The electrostatic LbL assembly can also be used to tune surface charges. For example, it has been reported that polyelectrolyte layers may be assembled on colloidal silica at different pH values, after which the ζ potential was determined as a function of the solution pH to obtain the local apparent dissociation constants of each surface layer.[34,35] The Rubner group acidified polyelectrolyte multilayers using weak polycation components in their assembly to expose mobile cationic charges, which were responsible for antibacterial properties of the surface.[36] However, manipulation of the surface charge on a flat surface using the LbL method, resulting in a controlled shift of the IEPs, has not been reported. Moreover, ζ potential-tuned LbL systems have not been reported in the context of antifouling research.

The LbL films can serve as a versatile platform to prepare antifouling materials.[37] Surface characteristics of the films can be easily adjusted by the choice of the materials used and by the parameters of the deposition process.[38,39] The physical properties of the multilayers such as thickness, mechanical characteristic, and surface charge can be manipulated by changing the pH and ionic strength of the polymer solution.[37,40] The thickness of LbL polyelectrolyte films can be controlled by pH adjustment of the solution of weak polyelectrolytes by changing the degree of ionization of the corresponding polyions.[41−43] Poly(allylamine hydrochloride)/Poly(acrylic acid) (PAH/PAA) thin multilayers constructed at high pH were reported to attract highly adhesive, murine fibroblast NR6WT cells. On the other hand, thick PAH/PAA multilayers constructed at low pH values swell substantially in physiological conditions and form highly hydrated surfaces. These layers resisted fibroblast attachment.[44]

Bulk LbL films are typically charge balanced, nevertheless the top layer of the film is charge overcompensated and can prevent, or promote, protein adsorption through electrostatic interactions.[45] It is also well documented that positively charged surfaces may kill bacteria.[37] PAH and poly(sodium 4-styrenesulfonate) (PSS) were assembled at high pH to incorporate uncharged amine groups into the LbL films, which were subsequently immersed in low pH solutions to induce base protonation, thus creating a multilayer system with sufficient activity to kill bacteria.[36] LbL films terminated by polycations have been reported to reduce the attachment of cyprids.[46] However, the behavior of foulants on planar LbL film surfaces with precisely defined ζ potential at a working pH has not been demonstrated.

In this study, we present a comprehensive set of protocols to fine-tune surface ζ potentials of LbL structures on planar substrates. As a demonstration of the broad control of the film properties, surfaces with isoelectric point values (IEP) ranging from 6 to 10 using typical polyelectrolytes were prepared. Importantly, the presented strategy allowed us to independently tune the surface ζ potential without changing chemical composition of the top layer. Thus, effective decoupling of the surface charge from other surface properties is possible by this design. Bioassays employing fouling organisms like barnacle cyprids and bacteria were conducted to demonstrate the high correlation between fouling prevention properties of LbL surfaces and their ζ potentials.

2. EXPERIMENTAL SECTION

2.1. Materials and Instruments. Poelectrolytes including PAA (M_w, ~450 000), poly(diallyldimethylammonium chloride) (PDADMAC; M_w: <100 000; 35 wt % in H_2O) and polyethylenimine (PEI; M_w, 25 000; branched) were provided by Sigma-Aldrich. (3-Aminopropyl)trimethoxysilane (APTMS, 97%) was also supplied by Sigma-Aldrich. Solvents including toluene, methanol, and ethanol were purchased from Tedia. Silicon wafers were obtained from Latech Scientific Supply, Pte., Ltd. Ultrapure water produced by a Millipore Milli-Q integral water purification system was used to prepare aqueous solutions. A triple P plasma processor (Duratek, Taiwan) was used to clean the silicon wafers.

2.2. Assembly of the LbL Films. Silicon wafers were cut into 2 × 2 cm slides using a DISCO dicing machine (DAD 321). After ultrasonic cleaning with water and ethanol for 10 min, the slides were dried over a nitrogen gas stream and treated by oxygen plasma (200 W) for 2 min. The treated silicon wafers were immersed into 3-aminopropyltrimethoxysilane toluene solutions (10 mM) for 5 h to impart positively charged amine groups on the substrate surface.

The pretreated silicon wafer slides were immersed into aqueous polyanion solutions (1 mg/mL) for 10 min and then rinsed with ultrapure water for 2 min. Subsequently, slides were immersed into polycation aqueous solutions (1 mg/mL) for 10 min, followed by ultrapure water rinse for another 2 min. The cycle was repeated until the desired bilayer number was reached. The pH values of the polyelectrolyte solutions were well controlled. The silicon wafers with the deposited LbL films were dried by nitrogen stream and later under vacuum at room temperature for 5 h. The prepared LbL films were stored in a desiccator prior to further use.

2.3. Characterization of the LbL Assemblies. Surface morphology and thickness of the prepared LbL films were measured by a JPK, NanoWizard 3 NanoOptics atomic force microscope (AFM) system in the "AC mode" (tapping mode). In AFM measurements, Tap300AI-G cantilevers made by Budget Sensors were used. AFM images were taken on dried films over scan areas of 2 × 2 μm for morphology observations and roughness measurements. The film thickness was measured by scratching the multilayer assembly with a fresh razor blade to expose the bare substrate (silicon) and then scanning the sample over 10 × 10 μm to reveal a clear step obtained by the scratch.[47] Five sections crossing the step of a single scratch were used to measure the height differences. The mean value of the height differences obtained was used as the film thickness value. The AFM raw data were processed by the software of the instrument provider (JPK Data Processing, 4.3.25).

The wetting properties of the deposited LbL films were evaluated by water contact angle measurements. A goniometer (250-F1) from Ramé-Hart Instrument Co. was used to measure the contact angles by the static sessile drop method. The silicon substrate wafers with the LbL films were mounted on flat holders. A 5 μL droplet of water was dispensed onto the dry sample surface by using a microsyringe. The water droplet image was captured and analyzed by the instrument to obtain the contact angle value of the surface tested. For each sample, 10 measurements of water contact angles at different locations on the LbL film surface were made, and the average value of the measurements was used as the representative water contact angle of the film.

Values of ζ potentials of the flat surfaces were measured with a SurPASS electrokinetic analyzer from Anton Paar. Silicon wafers with various LbL films were cut into 1 × 2 cm slides. Two slides were attached to the sample holders, which were inserted into the adjustable gap cell of SurPASS. After adjusting the gap height between the slides to 100 μm, the ζ potential measurement was conducted in 0.001 M KCl aqueous solution with auto pH titration from 10 to 5.5 by adding 0.05 M HCl aqueous solution. Because the slides were smooth and had a known surface area, the streaming current mode was used.

2.4. Biofouling Tests. *2.4.1. Barnacle Settlement Assay.* *Amphibalanus amphitrite* barnacle larvae were spawned from adults collected from the Kranji mangrove, Singapore. The nauplius larvae were fed with an algal mixture of 1:1 v/v of *Tetraselmissuecica* (CSIRO strain number CS-187) and *Chaetocerosmuelleri* (CSIRO strain number CS-176) at a density of about 5 × 10^5 /mL and reared at 27 °C in 0.2 μm of filtered seawater with 2.7% salinity. Nauplii metamorphosed into cyprids in 5 days, and cyprids were aged for minimum of 2 days at 4−6 °C prior to use in settlement assays.[48] The cyprid settlement assay was carried out using the droplet method.[15] A 300 μL droplet of seawater containing 15−25 cyprids was dispensed onto the modified silica substrate for these tests. The experiment was conducted in the dark at 25 °C for 24 h. After 24 h, the total number and the number of settled cyprids were enumerated under an optical microscope. For each type of LbL film, five replicates were used, and the average settlement was recorded. The cyprid mortality results were analyzed with One-Way Analysis Variance (ANOVA), followed by a Tukey post-test. Data comparison was performed using GraphPad Prism 5 (GraphPad Software, Inc.). For all comparisons, values of $p \leq 0.05$ were considered as statistically significant.

2.4.2. Measurement of Adhesion Force between Cyprid Footprint Proteins on a Colloidal Probe on Selected Surfaces by AFM. Adhesion force measurements were carried out following a previously reported protocol.[49] The colloidal contact probes with SiO_2 spheres (NT-MDT) were covalently immobilized with cyprid footprint proteins using glutaraldehyde. The modified probe was used to approach the LbL film surface, and the adhesion force between the probe and the surface was subsequently measured by a JPK, NanoWizard 3 NanoOptics atomic force microscope (AFM) system. All force measurements were carried out in a filtered seawater environment (pH 8).

2.4.3. Amphora Adhesion Assay. *Amphora* species are the most commonly encountered raphid diatoms found in biofilms on submerged surfaces, and as such, they are often used in antifouling tests.[50] *Amphora coffeaeformis* (UTEX reference number B2080) was maintained in F/2 medium[51] in tissue culture flasks at 24 °C under a 12 h light/12 h dark regime for at least a week prior to use. The algae were gently removed from culture flasks with a cell scraper, and clumps were broken up by continuous pipetting and filtering through a 35 μm nitex mesh. The cell count was determined with a hemocytometer and a suspension containing 10 000 cells per mL was made up in 3% salinity, 0.22 μm filtered seawater (FSW). Silicon wafer controls and silicon wafers with LbL films were placed randomly in each well, in six-well Nunc multiwell culture plates, with eight replicates for each treatment. To each well, 5 mL of algal cell suspension was added. The experiment was incubated for 24 h in a 12 h light/12 h dark cycle at 24 °C. At the end of the incubation period, all slides were gently dipped in a beaker of 3% salinity, 0.22 μm FSW to rinse off any unattached cells. The rinsing step was repeated three times, and the slides were then air-dried. The slides were examined under an epi-fluorescence microscope. Ten random fields of view were scored at 20× magnifications (0.916 mm^2 per field of view) for each slide. The *Amphora* settlement results were analyzed with One-Way ANOVA, followed by a Tukey post-test. Data comparison was performed using GraphPad Prism 5 (GraphPad Software Inc.). For all comparisons, values of $p \leq 0.05$ were considered as statistically significant.

2.4.4. Bacteria Adhesion Assay. Three bacterial strains were used for the antibacterial tests. Marine bacterial *Pseudomonas* strain NCIMB

Scheme 1. Preparation of LbL Films and ζ Potential Values of Two Representative Surfaces at a Certain pH[a]

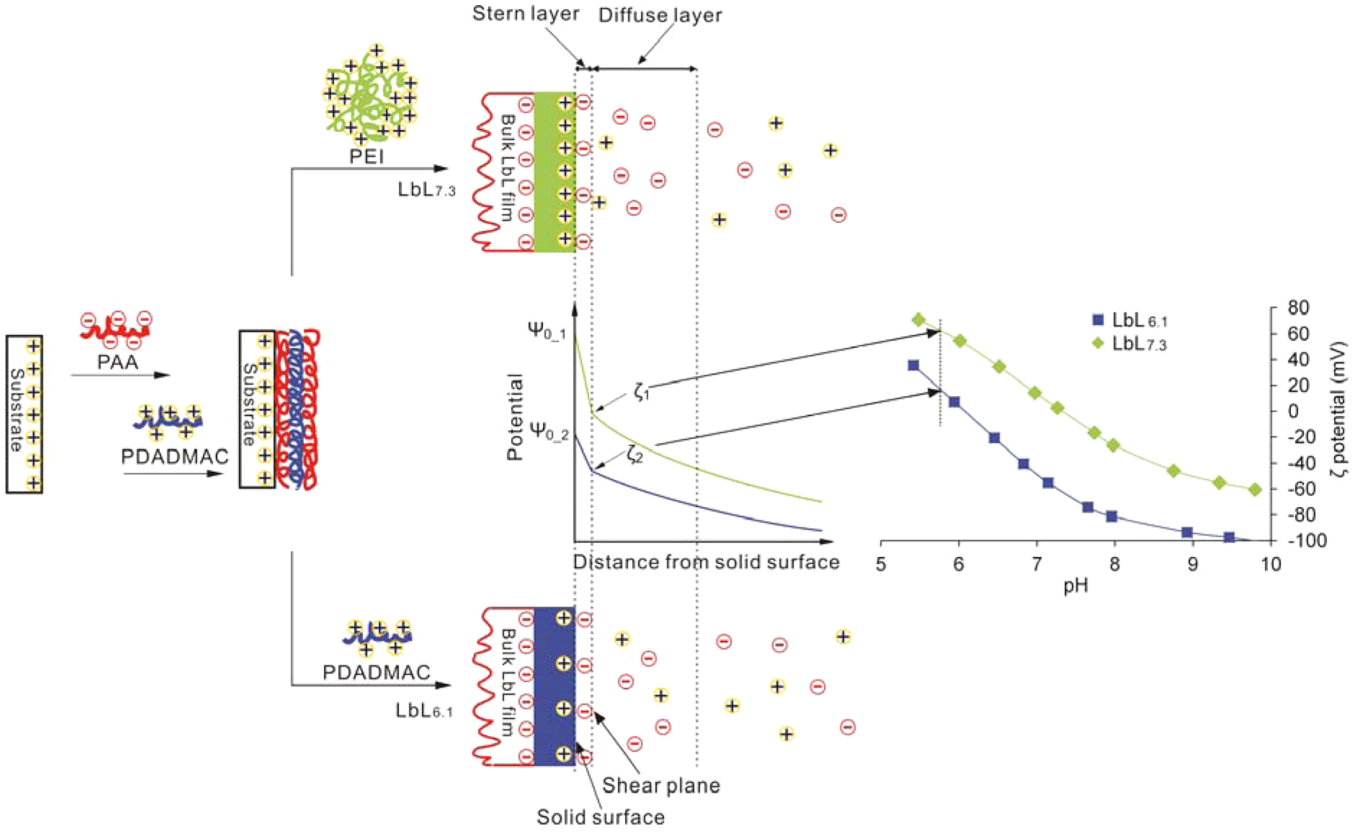

[a] ψ_{0_1} and ψ_{0_2} are the surface potentials of $LbL_{7.3}$ and $LbL_{6.1}$, respectively; ζ_1 and ζ_2 are the ζ potentials of $LbL_{7.3}$ and $LbL_{6.1}$, respectively.

2021 was obtained from the National Collection of Marine Bacteria (Sussex, U.K.) and cultured in a Marine Broth 2216 solution (37.4 g/L, Difco) at 25 °C.[48] *Escherichia coli* DH5 (*E. coli*, ATCC# 53868) and *Staphylococcus aureus* (*S. aureus*, ATTC# 25923) were obtained from American Type Culture Collection (ATCC, Manassas, VA). The two latter bacterial strains were cultivated in LB broth (10 g of tryptone, 5 g of yeast extract, and 10 g of NaCl) at 37 °C. The bacteria were cultured for about 16 h before harvest. The bacteria-containing broth was centrifuged at 3000 rpm for 10 min, and after the removal of the supernatant, the cells were washed twice and resuspended with sterile artificial seawater (ASW, pH 8) for *Pseudomonas* NCIMB 2021 and phosphate-buffered saline (PBS, pH 7.4) solution for *E. coli* and *S. aureus*.

After being incubated with bacterial suspension for 1 h, the samples were washed three times with PBS before fixing with 3% glutaraldehyde for 5 h at 4 °C. After the fixation, substrates were rinsed with DI water to remove the remaining glutaraldehyde and then dried at 60 °C in the oven for 24 h. The dried samples were coated with gold and then imaged with a scanning electron microscope (SEM, JEOL JSM-5600LV).

The surface coverage of bacteria was estimated by image analysis of the SEM micrographs with the ImageJ program (available as a public domain Java image processing program provided by the U.S. National Institute of Health). The total area covered by the bacteria clusters was calculated, and then divided by the total area of the image to give the percentage coverage of bacteria on the silicon wafer surface. The bacteria coverage for each sample was calculated based on 10 images obtained at different locations. Three samples were measured for each type of surfaces to get the average bacteria coverage. Plasma cleaned silicon wafers were also measured as a reference surface for adhesion testing.

3. RESULTS AND DISCUSSION

3.1. Tuning the Surface Charge of LbL Films. The general process for the LbL film preparation and its ζ potential control is shown in Scheme1. Following the Stern model,[52] the ζ potential on the shear plane of the electric double layer was measured in electrolyte solutions with different pH values (Scheme 1). In a typical scenario, when the surface charge is derived from the ionization of functional groups present at the interphase, the ζ potential decreases with increasing pH of the solution to which the surface is exposed.[53] As a consequence, the observed surface charge is variable and dependent on the ambient environmental conditions. For example, a material reaching the IEP with zero net charge in physiological environments (pH 7.4) is likely to be negatively charged in the marine environment (pH 8). As such, precise tuning of surface charge at a working pH helps to control attachment of various charged foulers.

In order to fabricate materials with controlled IEPs in a broad range, we propose three methods here (Scheme 2, Table 1). The methods described are based on a bulk model film constructed with PDADMAC/PAA. This polyelectrolyte couple was chosen based on the initial screening of various LbL components, as described in the Supporting Information.

3.1.1. Variation of the Polymer Amount Deposited by Adjusting Its Ionization Degree. In this approach, the ζ potential of the thin LbL film was controlled by adjusting the pH value of deposited materials across all layers (Scheme 2a). This method was derived from previously reported contributions linking the degree of ionization of the polyelectrolytes to the thickness of the films.[41,42] Six bilayers composed of PAA

dx.doi.org/10.1021/am507371a | ACS Appl. Mater. Interfaces 2015, 7, 852−861

Scheme 2. LbL Films Prepared From (d) PAA, PDADMAC, and PEI with Different Surface Charges Tuned by (a) Variation of the Polymer Amount Deposited by Adjusting Its Ionization Degree, (b) Modification of the Last Layer, and (c) Modification of the Penultimate Layer

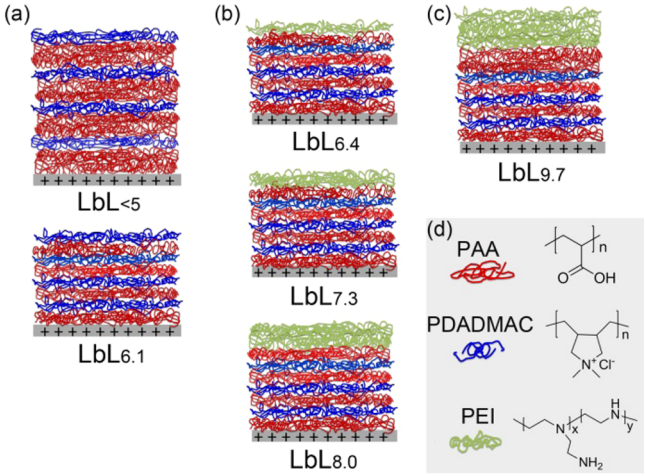

and PDADMAC were deposited at pH values 3 and 10 to fabricate the films $LbL_{<5}$ and $LbL_{6.1}$, respectively. Similar methods have been reported to assemble polyelectrolyte multilayers on colloidal silica to tune surface charges.[34,35]

As shown in Figure 1a, $LbL_{<5}$ prepared from the polyelectrolyte solutions at pH 3 has a negative ζ potential in the pH range between 5 and 10; i.e. it exhibits an IEP at a pH value less than 5. During deposition, when the pH value of polyelectrolyte solutions was increased to 10, the resulting IEP of the film was shifted to 6.1 ($LbL_{6.1}$). The cationic polyelectrolyte PDADMAC bears permanently charged quaternary ammonium groups, with ionization which is not sensitive to pH. However, PAA, which is a weak polyacid with pK_a = 4.5,[54] includes carboxylic groups and its degree of ionization is determined by the pH. When PAA was assembled at pH 3, the majority of its carboxyl groups were not ionized (~97%), and as such more PAA was deposited to compensate the positive charges from the underlying polycation layer. These assembled but not fully ionized carboxyl groups of PAA will be deprotonated upon exposure of LbL to the higher pH solution, resulting in the overall highly negative ζ potential of the $LbL_{<5}$ film. As expected on the basis of the arguments above, the ionization degree of PAA increases with pH, and as a result, lower amounts of PAA are deposited to compensate the

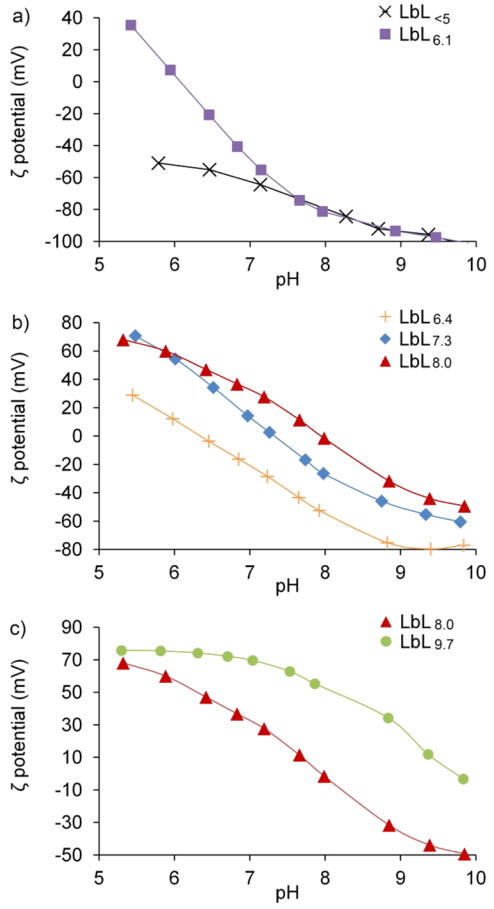

Figure 1. The ζ potentials of LbL films prepared using different surface charge tuning methods including (a) variation of the polymer amount deposited by adjusting its ionization degree, (b) modification of the last layer, and (c) modification of the penultimate layer.

underlying positive charges at a higher assembly pH. Thus, the $LbL_{6.1}$ film assembled at pH 10 indicated an obviously higher IEP at 6.1 due to the lower load of the PAA in the film. In short, in the PAA and PDADMAC LbL systems, higher assembly pH results in less negative charges, or a higher IEP, for the LbL film. However, this approach has limitations for IEP control. For the deposition pH much higher than the pK_a of PAA, the polyanion component is completely ionized.[42] As such the PAA/PDADMAC film with the highest IEP achievable using the method was 6.1. Unfortunately, a surface with an IEP

Table 1. Polyelectrolyte Solutions Used to Prepare LbL Films

tuning method	LbL films	IEP	polyanion and pH for the first five bilayers	polycation and pH for the first five bilayers	polyanion and pH for the penultimate layer	polycation and pH for the last layer
variation of the polymer amount deposited by adjusting its ionization degree	$LbL_{<5}$	<5	PAA, 3	PDADMAC, 3	PAA, 3	PDADMAC, 3
	$LbL_{6.1}$	6.1	PAA, 10	PDADMAC, 10	PAA, 10	PDADMAC, 10
modification of the last layer	$LbL_{6.4}$	6.4	PAA, 10	PDADMAC, 10	PAA, 10	PEI, 8.5
	$LbL_{7.3}$	7.3	PAA, 10	PDADMAC, 10	PAA, 10	PEI, 10
	$LbL_{8.0}$	8.0	PAA, 10	PDADMAC, 10	PAA, 10	PEI, 10.5
modification of the penultimate layer	$LbL_{9.7}$	9.7	PAA, 10	PDADMAC, 10	PAA, 3	PEI, 10.5

dx.doi.org/10.1021/am507371a | ACS Appl. Mater. Interfaces 2015, 7, 852−861

at 6.1 would still be negatively charged in typical biomedical and marine environments.

3.1.2. Modification of the Last Layer. To prepare LbL films that maintain a charge-compensated structure at higher pH values, we chose to modify the last layer by the exchange of PDADMAC to a polycation with tunable ionization properties, namely, PEI.[53] PEI is a basic polymer bearing primary and secondary amines with ionization degrees that are pH-dependent.

The bulk film (5.5 bilayers) was built up with the PAA and PDADMAC solutions at pH 10, as described earlier. Subsequently, the top layer of the film was fabricated using PEI solutions characterized with different pH values (Scheme 2b). The $LbL_{6.4}$ film deposited at pH 8.5 exhibited an IEP at 6.4. When the assembly pH of PEI last layer was increased to 10, the IEP was shifted to 7.3 ($LbL_{7.3}$) and finally to 8 ($LbL_{8.0}$) when PEI as the last layer was deposited at pH 10.5 (Figure 1b).With the increase of assembly pH, PEI ionization was lowered, and more molecules were needed to compensate the negative charge of the underlying layers. Greater amounts of amine deposited as a top layer resulted in a shift in the IEP of the film to higher values.

The described deposition of PEI at pH > 10.5 is problematic because the majority of functional groups are not protonated under those conditions. The threshold backbone charge density requirement, necessary to overcome the entropic loss of adsorption, is not met.[55] Accumulation can still be observed as a result of H-bonding between amine proton donors ($-NH_2$ or $-NH$) and carbonyl group (C═O) acceptors formed at high pH values.[56] This H-bonded PEI layer is, however, easily removed by immersion in seawater or with a high-pressure rinse using KCl solutions in the streaming potential measurement device. As such, the highest IEP of stable LbL film achievable following this method is approximately 8.

3.1.3. Modification of the Penultimate Layer. To fabricate stable LbL films with IEPs shifted further to higher values, elements of the first method (variation of the polymer amount deposited by adjusting its ionization degree) and the second method (modification of the last layer) were combined. Similarly, the first five bilayers of the $LbL_{9.7}$ film were assembled in PAA and PDADMAC solutions of pH 10. Subsequently, PAA in the penultimate layer was deposited at pH 3. Finally, the PEI in the last layer was assembled at pH 10.5. Following this approach, it is possible to fabricate an LbL film with an isoelectric point as high as 9.7 (Scheme 2c, Figure 1c).

The quantity of PEI deposited in the last layer, which determines the surface charge and IEP of the LbL film, can be fine-tuned not only by adjusting the assembly pH of PEI for the top layer, but also by tuning the amount of deposited PAA for the penultimate layer. Low assembly pH used for the deposition of PAA in the penultimate layer resulted in a high polymer load. This subsequently attracts additional PEI during the final PEI deposition step at the high pH, forming the last layer of $LbL_{9.7}$ and pushing the IEP of fabricated surfaces to 9.7.

3.2. Antifouling Evaluation of LbL Surfaces with Precisely Tuned ζ Potential Values. The development of the LbL engineering methods described in this work was primarily motivated to provide model surfaces for studies of the correlation of fouling with the ζ potential of the substrates. The surface charge tuning methodologies presented allowed us to prepare LbL films with zero net charge or IEP at any pH value between 6 and 10. This covers a range of environmental conditions that typical antifouling technologies face. As shown in Figure 2, the ζ potential of $LbL_{7.3}$ and $LbL_{8.0}$ were adjusted

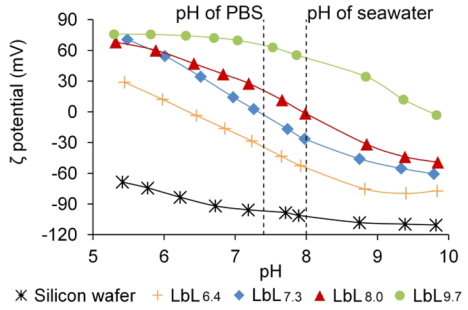

Figure 2. The ζ potentials of the selected LbL films at target pH values.

to zero at pH 7.4, which is a typical pH value for most physiological fluids,[57] and at pH 8, which is a pH of typical marine environment,[58] respectively. These surfaces were used to carry out a series of tests with different foulants. In addition, one negatively charged $LbL_{6.4}$ film and one positively charged $LbL_{9.7}$ film were prepared to complete the series. A plasma-cleaned bare silicon wafer was employed as the control surface.

As shown in Table 2, all films investigated were hydrophilic and showed similar water contact angles at around 40°. The $LbL_{6.4}$, $LbL_{7.3}$, and $LbL_{8.0}$ films showed similar thicknesses (15 nm); only the $LbL_{9.7}$ film displayed a higher thickness (40 nm). The thickness of $LbL_{9.7}$ was increased due to the high quantity of PAA in the penultimate layer and the resulting PEI amount in the last layer. As shown in Figure 3, the surfaces of the selected LbL films were smooth and exhibited roughness values lower than 1 nm. The first five bilayers of the selected LbL films were identical and composed of PAA and PDADMAC. The top layer was always composed of PEI, providing the identical chemical composition of the film exposed to the fouling environment. Identical surface chemistry of the top layer and similar hydrophilicity and roughness minimized the influences of the other factors besides the surface charge. Thus, these films are excellent candidates to decouple the influence of surface charge and other parameters influencing adhesion, for fouling studies.

3.2.1. Marine Antifouling Tests. Barnacle cyprids are widely used to evaluate the antifouling performance of various coatings.[59] In this study, the settled and the dead cyprids on negatively charged ($LbL_{6.4}$), neutral ($LbL_{8.0}$), and positively charged ($LbL_{9.7}$) films were counted after 24 h of incubation. As shown in Figure 4a, approximately 50% of cyprids settled on the negatively charged $LbL_{6.4}$ surface and on the control surface (plasma-cleaned silicon wafer). Less than 10% of cyprids settled on the zero net charge $LbL_{8.0}$. The lowest settlement was observed on the positively charged $LbL_{9.7}$ film. The fraction of dead cyprids on each LbL film was not significantly different, as compared to the control surface (One-Way ANOVA, $p > 0.05$), indicating that the selected LbL films are not toxic.

The cyprid settlement results clearly show that cyprids prefer to settle on negatively charged surfaces, rather than on the neutral or positively charged surfaces. We note that a similar result was reported previously by the Liedberg group using SAMs as substrates.[16]

To verify the mechanism of the cyprid settlement behavior, we investigated the interaction between the cyprid's footprint proteins (i.e. protein secretion deposited at barnacle larval

dx.doi.org/10.1021/am507371a | ACS Appl. Mater. Interfaces 2015, 7, 852−861

Table 2. Characteristics of the Selected LbL Films

surfaces	silicon wafer	$LbL_{6.4}$	$LbL_{7.3}$	$LbL_{8.0}$	$LbL_{9.7}$
water contact angle (deg)	<15	41 ± 2	42 ± 1	43 ± 1	36 ± 3
thickness (nm)	0	10.0 ± 0.8	15.3 ± 1.5	18.4 ± 1.2	40.1 ± 3.6
roughness (Ra, nm)	0.2	0.6	0.5	0.7	0.4

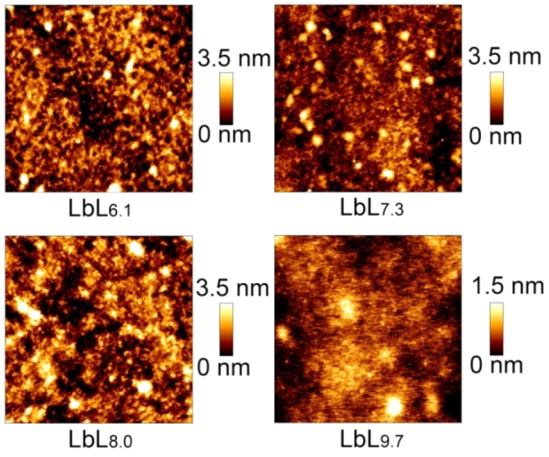

Figure 3. AFM height images of the selected LbL films. Scan size: 2 μm × 2 μm.

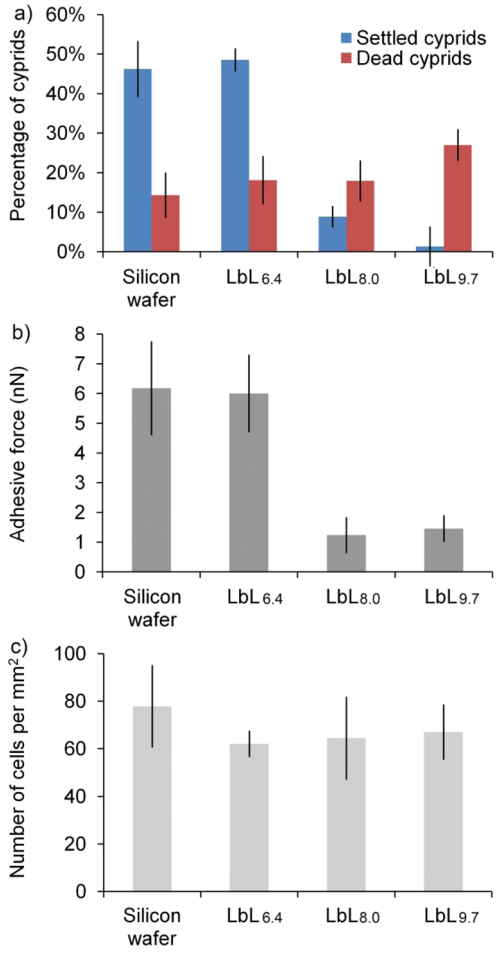

Figure 4. Marine antifouling tests including (a) cyprid settlement, (b) cyprid footprint protein adhesion from AFM experiments, and (c) *Amphora* settlement on the selected LbL films with different charges. Error bars correspond to standard deviations.

stage) and the selected surfaces using AFM in an aqueous environment. Colloidal AFM probes were covalently functionalized with cyprid's footprint proteins and subsequently used to probe the model surfaces following our recently established protocol.[49] As shown in Figure 4b, the footprint proteins display a strong adhesion to the negatively charged samples ($LbL_{6.4}$ and control). Much lower adhesion forces were observed between the proteins and the zero net charge surface $LbL_{8.0}$, as well as the positively charged $LbL_{9.7}$ film. Footprint adhesion results in this case correlate well with the cyprid settlement data. These results suggest that the interaction between the settlement adhesion proteins and the negatively charged surfaces were much stronger than the interactions for neutral and positively charged samples. Because other parameters such as hydrophilicity and roughness were well controlled and essentially identical for the surfaces studied, the results presented here strongly indicate that the footprint proteins of cyprids are net charge positive in the marine environment.

Not every tested organism responded to changes in the ζ potential of our model surfaces. In *Amphora* adhesion tests, the attached cell density differences among the selected LbL films were not significant (One-Way ANOVA, $p > 0.05$, Figure 4c). We may conclude that the settlement of *Amphora* is not significantly affected by electrostatic interactions in the investigated range of IEPs.

3.2.2. Bacteria Adhesion Tests. *Pseudomonas* (NCIMB 2021), a marine bacterium isolated from a marine biofilm, was used to test the neutral ($LbL_{8.0}$), negatively charged ($LbL_{6.4}$), and positively charged ($LbL_{9.7}$) films in artificial seawater at pH 8. *Pseudomonas* is present in most environments and is identified as one of the most common bacteria associated with biofouling due to its extracellular polysaccharide (EPS) secretions. We note that *Pseudomonas* species have often been used to examine biofouling processes in model studies.[61]

Because bacterial fouling is particularly relevant for biomedical applications, we used two common bacteria living in the physiological environment, that is *E. coli* (Gram negative) and *S. aureus* (Gram positive) to test the neutral ($LbL_{7.3}$), negatively charged ($LbL_{6.4}$), and positively charged ($LbL_{9.7}$) films in PBS (artificial physiological environment) at pH 7.4. Fouling tests of all listed microorganisms were carried out using a fixed settlement protocol and evaluated by SEM imaging.

Bacterial cell surfaces, due to ionized phosphoryl and carboxylate substituents on the outer cell envelope, possess net negative electrostatic charge.[62] As shown in Figure 5a, bacteria clusters covered more than 30% area of the positively charged surface ($LbL_{9.7}$) in 1 h. However, bacteria coverage on the neutral ($LbL_{8.0}$) and negatively charged ($LbL_{6.4}$) was lower, at about 13%. The lowest bacteria coverage was observed on the bare silicon surface at 2%. Numerous *Pseudomonas* (NCIMB 2021) cells were attracted to the $LbL_{9.7}$ surface by electrostatic force. A much lower number was settled on the neutral $LbL_{8.0}$ and negatively charged $LbL_{6.4}$; however, settlement was still clearly visible. This may be caused by EPS secreted by *Pseudomonas* (NCIMB 2021), which may

dx.doi.org/10.1021/am507371a | ACS Appl. Mater. Interfaces 2015, 7, 852−861

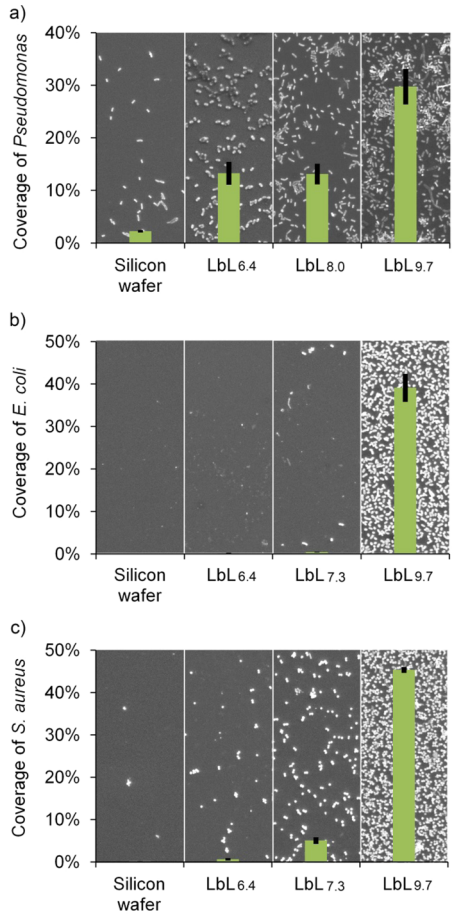

Figure 5. Bacteria coverage of the selected LbL films after (a) *Pseudomonas* (NCIMB 2021), (b) *E. coli*, and (c) *S. aureus* adhesion assays. Error bars correspond to standard deviations. Representative SEM micrographs set as a background for each experiment are 40 × 96 μm in size.

boost the nonspecific adhesion of bacteria onto various materials.[60]

E. coli (Gram negative) and *S. aureus* (Gram positive) adhesion showed a similar trend, as seen in Figure 5b,c. The *E. coli* and *S. aureus* coverage values on the $LbL_{9.7}$ were about 39 and 45%, respectively. Fewer *E. coli* (coverage at ~0%) and *S. aureus* (coverage at ~5%) were observed on the neutral $LbL_{7.3}$ surfaces. Almost no *E. coli* and *S. aureus* were found on the negatively charged $LbL_{6.4}$ film. The negatively charged bacteria including *E. coli* and *S. aureus* were attracted to the positively charged surface by electrostatic force but barely settled on the neutral surface and the negatively charged surface. These results demonstrate that the LbL films with zero net charge or negative charge can limit the adhesion of bacteria. The results presented are in good agreement with previously published reports on adhesion of microorganisms.[18]

4. CONCLUSIONS

Three methods for fine control of LbL film surface charge were established and applied for the fabrication of polyelectrolyte films with controlled IEP values. In the LbL systems of this study, PAA as a weak polyelectrolyte and PDADMAC as a strong polyelectrolyte were used to build up the bulk films, and PEI as a weak polyelectrolyte was applied as top layer for some films. The tuning methods of surface charge rely on (1) changing the pH value of PAA and PDADMAC solutions to build up the bulk film, (2) tuning the pH of PEI deposited on the last layer, and (3) tuning the pH of PAA deposited on the penultimate layer. Following these methods, surfaces with a wide range of IEP from 6 to 10 were fabricated. The unique feature of this approach is that control over the surface ζ potential can be essentially decoupled from chemical properties of the top layer, and as such, the influence of a single surface parameter (charge) can be investigated. This is not the case when other surface modification methods (e.g., using mixed self-assembled monolayers) are used.

In marine antifouling tests, more cyprids settled on the negatively charged LbL surface than on the neutral and positively charged LbL films. We associate this with the net positive charge of the cyprid's footprint proteins, which was verified by assessing the adhesion of cyprid footprint proteins by employing footprint protein modified AFM colloidal probes. Reverse trends (high adhesion on positively charged surface but low on neutral and negatively charged surface) were observed in bacteria adhesion tests by using *Pseudomonas* (NCIMB 2021), *E. coli* (Gram negative), and *S. aureus* (Gram positive). This was attributed to the negative charge of the bacteria cell walls.

Several applications can be envisaged employing this technology such as selective adsorption or purification of proteins, adsorption or removal of metal ions from wastewater, preparation of artificially charged bacterial cell walls, and fabrication of charge controlled LbL capsules for drug delivery. This fabrication approach did not provide ultimate antifouling solutions, but rather, it offers some guiding principles to manipulate the IEP of LbL films. Additional steps such as cross-linking should be implemented to make LbL layers fully exploitable for marine or biomedical applications. Corresponding studies are in progress.

■ ASSOCIATED CONTENT

Supporting Information

Materials characterization, surface properties including roughness and water contact angle of the prepared LbL films, and results of initial antifouling prescreening using *Amphora* settlement test and various commercially available polyelectrolytes. This material is available free of charge via the Internet at http://pubs.acs.org.

■ AUTHOR INFORMATION

Corresponding Authors

*E-mail: dominik.janczewski@ch.pw.edu.pl. Tel: +48 22 234 5583. Fax: +48 22 234 5504.

*E-mail: g.j.vancso@utwente.nl. Tel.: +31 53 489 2974. Fax: +31 53 489 3823.

Present Address

⊥Laboratory of Technological Processes, Faculty of Chemistry, Warsaw University of Technology, Noakowskiego 3, 00-664 Warsaw, Poland

Notes

The authors declare no competing financial interest.

■ ACKNOWLEDGMENTS

The authors are grateful to the Agency for Science, Technology, and Research (A*STAR) for providing financial support under the Innovative Marine Antifouling Solutions (IMAS) program.

REFERENCES

(1) Banerjee, I.; Pangule, R. C.; Kane, R. S. Antifouling Coatings: Recent Developments in the Design of Surfaces That Prevent Fouling by Proteins, Bacteria, and Marine Organisms. *Adv. Mater.* **2011**, *23*, 690−718.

(2) Vasilev, K.; Cook, J.; Griesser, H. J. Antibacterial Surfaces for Biomedical Devices. *Expert Rev. Med. Devices* **2009**, *6*, 553−567.

(3) Rana, D.; Matsuura, T. Surface Modifications for Antifouling Membranes. *Chem. Rev.* **2010**, *110*, 2448−2471.

(4) Callow, J. A.; Callow, M. E. Trends in the Development of Environmentally Friendly Fouling-Resistant Marine Coatings. *Nat. Commun.* **2011**, *2*, 244.

(5) Hucknall, A.; Rangarajan, S.; Chilkoti, A. In Pursuit of Zero: Polymer Brushes that Resist the Adsorption of Proteins. *Adv. Mater.* **2009**, *21*, 2441−2446.

(6) Amiji, M.; Park, K. Surface Modification of Polymeric Biomaterials with Poly(ethylene oxide), Albumn, and Heparin for Reduced Thrombogenicity. *J. Biomater. Sci., Polym. Ed.* **1993**, *4*, 217−234.

(7) Lejars, M.; Margaillan, A.; Bressy, C. Fouling Release Coatings: A Nontoxic Alternative to Biocidal Antifouling Coatings. *Chem. Rev.* **2012**, *112*, 4347−4390.

(8) Salta, M.; Wharton, J. A.; Stoodley, P.; Dennington, S. P.; Goodes, L. R.; Werwinski, S.; Mart, U.; Wood, R. J. K.; Stokes, K. R. Designing Biomimetic Antifouling Surfaces. *Philos. Trans. R. Soc., A* **2010**, *368*, 4729−4754.

(9) Schultz, M. P.; Bendick, J. A.; Holm, E. R.; Hertel, W. M. Economic Impact of Biofouling on a Naval Surface Ship. *Biofouling* **2011**, *27*, 87−98.

(10) Krishnan, S.; Weinman, C. J.; Ober, C. K. Advances in Polymers for Anti-Biofouling Surfaces. *J. Mater. Chem.* **2008**, *18*, 3405−3413.

(11) Schumacher, J. F.; Carman, M. L.; Estes, T. G.; Feinberg, A. W.; Wilson, L. H.; Callow, M. E.; Callow, J. A.; Finlay, J. A.; Brennan, A. B. Engineered Antifouling Microtopographies-Effect of Feature Size, Geometry, and Roughness on Settlement of Zoospores of the Green Alga Ulva. *Biofouling* **2007**, *23*, 55−62.

(12) Verran, J.; Boyd, R. D. The Relationship between Substratum Surface Roughness and Microbiological and Organic Soiling: A Review. *Biofouling* **2001**, *17*, 59−71.

(13) Lindner, E. A Low Surface Free Energy Approach in the Control of Marine Biofouling. *Biofouling* **1992**, *6*, 193−205.

(14) Zhu, X.; Guo, S.; Janczewski, D.; Velandia, F. J. P.; Teo, S. L.-M.; Vancso, G. J. Multilayers of Fluorinated Amphiphilic Polyions for Marine Fouling Prevention. *Langmuir* **2014**, *30*, 288−296.

(15) Finlay, J. A.; Bennett, S. M.; Brewer, L. H.; Sokolova, A.; Clay, G.; Gunari, N.; Meyer, A. E.; Walker, G. C.; Wendt, D. E.; Callow, M. E.; Callow, J. A.; Detty, M. R. Barnacle Settlement and the Adhesion of Protein and Diatom Microfouling to Xerogel Films with Varying Surface Energy and Water Wettability. *Biofouling* **2010**, *26*, 657−666.

(16) Petrone, L.; Di Fino, A.; Aldred, N.; Sukkaew, P.; Ederth, T.; Clare, A. S.; Liedberg, B. Effects of Surface Charge and Gibbs Surface Energy on the Settlement Behaviour of Barnacle Cyprids (*Balanus amphitrite*). *Biofouling* **2011**, *27*, 1043−1055.

(17) Abarzua, S.; Jakubowski, S. Biotechnological Investigation for the Prevention of Biofouling. I. Biological and Biochemical Principles for the Prevention of Biofouling. *Mar. Ecol.: Prog. Ser.* **1995**, *123*, 301−312.

(18) Zhao, Y. H.; Zhu, X. Y.; Wee, K. H.; Bai, R. Achieving Highly Effective Non-Biofouling Performance for Polypropylene Membranes Modified by UV-Induced Surface Graft Polymerization of Two Oppositely Charged Monomers. *J. Phys. Chem. B* **2010**, *114*, 2422−2429.

(19) Holmlin, R. E.; Chen, X. X.; Chapman, R. G.; Takayama, S.; Whitesides, G. M. Zwitterionic SAMs that Resist Nonspecific Adsorption of Protein from Aqueous Buffer. *Langmuir* **2001**, *17*, 2841−2850.

(20) Delgado, Á. V.; Arroyo, F. Electrokinetic Phenomena and Their Experimental Determination: An Overview. In *Interfacial Electrokinetics and Electrophoresis*, Delgado, Á. V., Ed. Marcel Dekker: New York, 2002; p 1−54.

(21) Kang, M. S.; Chun, B.; Kim, S. S. Surface Modification of Polypropylene Membrane by Low-Temperature Plasma Treatment. *J. Appl. Polym. Sci.* **2001**, *81*, 1555−1566.

(22) Wong, I.; Ho, C.-M. Surface Molecular Property Modifications for Poly(dimethylsiloxane) (PDMS) Based Microfluidic Devices. *Microfluid. Nanofluid.* **2009**, *7*, 291−306.

(23) Chen, S.; Yu, F.; Yu, Q.; He, Y.; Jiang, S. Strong Resistance of a Thin Crystalline Layer of Balanced Charged Groups to Protein Adsorption. *Langmuir* **2006**, *22*, 8186−8191.

(24) Mi, L.; Bernards, M. T.; Cheng, G.; Yu, Q.; Jiang, S. pH Responsive Properties of Non-Fouling Mixed-Charge Polymer Brushes Based on Quaternary Amine and Carboxylic Acid Monomers. *Biomaterials* **2010**, *31*, 2919−2925.

(25) Quintana, R.; Gosa, M.; Jańczewski, D.; Kutnyanszky, E.; Vancso, G. J. Enhanced Stability of Low Fouling Zwitterionic Polymer Brushes in Seawater with Diblock Architecture. *Langmuir* **2013**, *29*, 10859−10867.

(26) Chen, S.; Jiang, S. A New Avenue to Nonfouling Materials. *Adv. Mater.* **2008**, *20*, 335−338.

(27) Ariga, K.; Yamauchi, Y.; Rydzek, G.; Ji, Q.; Yonamine, Y.; Wu, K. C. W.; Hill, J. P. Layer-by-Layer Nanoarchitectonics: Invention, Innovation, and Evolution. *Chem. Lett.* **2014**, *43*, 36−68.

(28) Decher, G. Fuzzy Nanoassemblies: Toward Layered Polymeric Multicomposites. *Science* **1997**, *277*, 1232−1237.

(29) Decher, G.; Schlenoff, J. B. *Multilayer Thin Films: Sequential Assembly of Nanocomposite Materials*. Wiley-VCH: Weinheim, 2006.

(30) Song, J.; Janczewski, D.; Guo, Y.; Xu, J.; Vancso, G. J. Redox Responsive Nanotubes from Organometallic Polymers by Template Assisted Layer by Layer Fabrication. *Nanoscale* **2013**, *5*, 11692−11698.

(31) De Cock, L. J.; De Koker, S.; De Geest, B. G.; Grooten, J.; Vervaet, C.; Remon, J. P.; Sukhorukov, G. B.; Antipina, M. N. Polymeric Multilayer Capsules in Drug Delivery. *Angew. Chem., Int. Ed.* **2010**, *49*, 6954−6973.

(32) Kozlovskaya, V.; Ok, S.; Sousa, A.; Libera, M.; Sukhishvili, S. A. Hydrogen-Bonded Polymer Capsules Formed by Layer-by-Layer Self-Assembly. *Macromolecules* **2003**, *36*, 8590−8592.

(33) Izquierdo, A.; Ono, S. S.; Voegel, J. C.; Schaaf, P.; Decher, G. Dipping versus Spraying: Exploring the Deposition Conditions for Speeding up Layer-by-Layer Assembly. *Langmuir* **2005**, *21*, 7558−7567.

(34) Burke, S. E.; Barrett, C. J. Acid-Base Equilibria of Weak Polyelectrolytes in Multilayer Thin Films. *Langmuir* **2003**, *19*, 3297−3303.

(35) Burke, S. E.; Barrett, C. J. pH-Responsive Properties of Multilayered Poly(L-lysine)/Hyaluronic Acid Surfaces. *Biomacromolecules* **2003**, *4*, 1773−1783.

(36) Lichter, J. A.; Rubner, M. F. Polyelectrolyte Multilayers with Intrinsic Antimicrobial Functionality: The Importance of Mobile Polycations. *Langmuir* **2009**, *25*, 7686−7694.

(37) Lichter, J. A.; Van Vliet, K. J.; Rubner, M. F., Design of Antibacterial Surfaces and Interfaces: Polyelectrolyte Multilayers as a Multifunctional Platform. *Macromolecules* **2009**, *42*.

(38) Kuo, W. H.; Wang, M. J.; Chien, H. W.; Wei, T. C.; Lee, C.; Tsai, W. B. Surface Modification with Poly(sulfobetaine methacrylate-co-acrylic acid) To Reduce Fibrinogen Adsorption, Platelet Adhesion, and Plasma Coagulation. *Biomacromolecules* **2011**, *12*, 4348−4356.

(39) Cortez, C.; Quinn, J. F.; Hao, X.; Gudipati, C. S.; Stenzel, M. H.; Davis, T. P.; Caruso, F. Multilayer Buildup and Biofouling Characteristics of PSS-b-PEG Containing Films. *Langmuir* **2010**, *26*, 9720−9727.

(40) von Klitzing, R. Internal Structure of Polyelectrolyte Multilayer Assemblies. *Phys. Chem. Chem. Phys.* **2006**, *8*, 5012−5033.

(41) Yoo, D.; Shiratori, S. S.; Rubner, M. F. Controlling Bilayer Composition and Surface Wettability of Sequentially Adsorbed Multilayers of Weak Polyelectrolytes. *Macromolecules* **1998**, *31*, 4309−4318.

(42) Choi, J.; Rubner, M. F. Influence of the Degree of Ionization on Weak Polyelectrolyte Multilayer Assembly. *Macromolecules* **2005**, *38*, 116−124.
(43) Zhang, H. N.; Ruhe, J. Weak Polyelectrolyte Brushes as Substrates for the Formation of Surface-Attached Polyelectrolyte-Polyelectrolyte Complexes and Polyelectrolyte Multilayers. *Macromolecules* **2005**, *38*, 10743−10749.
(44) Mendelsohn, J. D.; Yang, S. Y.; Hiller, J.; Hochbaum, A. I.; Rubner, M. F. Rational Design of Cytophilic and Cytophobic Polyelectrolyte Multilayer Thin Films. *Biomacromolecules* **2003**, *4*, 96−106.
(45) Salloum, D. S.; Schlenoff, J. B. Protein Adsorption Modalities on Polyelectrolyte Multilayers. *Biomacromolecules* **2004**, *5*, 1089−1096.
(46) Zhu, X.; Jańczewski, D.; Lee, S. S. C.; Teo, S. L.-M.; Vancso, G. J. Cross-Linked Polyelectrolyte Multilayers for Marine Antifouling Applications. *ACS Appl. Mater. Interfaces* **2013**, *5*, 5961−5968.
(47) Lefaux, C. J.; Zimberlin, J. A.; Dobrynin, A. V.; Mather, P. T. Polyelectrolyte Spin Assembly: Influence of Ionic Strength on the Growth of Multilayered Thin Films. *J. Polym. Sci., Part B: Polym. Phys.* **2004**, *42*, 3654−3666.
(48) Willemsen, P. R.; Overbeke, K.; Suurmond, A. Repetitive Testing of TBTO, Sea-Nine 211 and Farnesol Using *Balanus amphitrite* (Darwin) Cypris Larvae: Variability in Larval Sensitivity. *Biofouling* **1998**, *12*, 133−147.
(49) Guo, S.; Puniredd, S. R.; Jańczewski, D.; Lee, S. S. C.; Teo, S. L. M.; He, T.; Zhu, X.; Vancso, G. J. Barnacle Larvae Exploring Surfaces with Variable Hydrophilicity: Influence of Morphology and Adhesion of "Footprint" Proteins by AFM. *ACS Appl. Mater. Interfaces* **2014**, *6*, 13667−13676.
(50) Holland, R.; Dugdale, T. M.; Wetherbee, R.; Brennan, A. B.; Finlay, J. A.; Callow, J. A.; Callow, M. E. Adhesion and Motility of Fouling Diatoms on a Silicone Elastomer. *Biofouling* **2004**, *20*, 323−329.
(51) Guillard, R. R.; Ryther, J. H. Studies of Marine Planktonic Diatoms 1. *Cyclotella nana* Hustedt and *Detonula confervacea* (Cleve) Gran. *Can. J. Microbiol.* **1962**, *8*, 229−239.
(52) Butt, H.-J.; Graf, K.; Kappl, M. *Physics and Chemistry of Interfaces*. Wiley-VCH: Weinheim, 2006; p 495.
(53) Kosmulski, M., Surface Charging and Points of Zero Charge. In *Surfactant Science Series 145* [Online] CRC Press: Boca Raton, FL, 2009.
(54) Gebhardt, J. E.; Fuerstenau, D. W. Adsorption of Polyacrylic-Acid at Oxide Water Interfaces. *Colloids Surf.* **1983**, *7*, 221−231.
(55) Shin, Y. W.; Roberts, J. E.; Santore, M. M. The Relationship between Polymer/Substrate Charge Density and Charge Overcompensation by Adsorbed Polyelectrolyte Layers. *J. Colloid Interface Sci.* **2002**, *247*, 220−230.
(56) Gowacki, E. D.; Irimia-Vladu, M.; Bauer, S.; Sariciftci, N. S. Hydrogen-Bonds in Molecular Solids—From Biological Systems to Organic Electronics. *J. Mater. Chem. B* **2013**, *1*, 3742−3753.
(57) Duprat, F.; Lesage, F.; Fink, M.; Reyes, R.; Heurteaux, C.; Lazdunski, M. TASK, A Human Background K+ Channel to Sense External pH Variations Near Physiological pH. *EMBO J.* **1997**, *16*, 5464−5471.
(58) Hansen, P. J. Effect of High pH on the Growth and Survival of Marine Phytoplankton: Implications for Species Succession. *Aquat. Microb. Ecol.* **2002**, *28*, 279−288.
(59) Holm, E. R. Barnacles and Biofouling. *Integr. Comp. Biol.* **2012**, *52*, 348−355.
(60) Pang, C. M.; Hong, P. Y.; Guo, H. L.; Liu, W. T. Biofilm Formation Characteristics of Bacterial Isolates Retrieved from a Reverse Osmosis Membrane. *Environ. Sci. Technol.* **2005**, *39*, 7541−7550.
(61) Al-Tahhan, R. A.; Sandrin, T. R.; Bodour, A. A.; Maier, R. M. Rhamnolipid-Induced Removal of Lipopolysaccharide from *Pseudomonas aeruginosa*: Effect on Cell Surface Properties and Interaction with Hydrophobic Substrates. *Appl. Environ. Microbiol.* **2000**, *66*, 3262−3268.
(62) Wilson, W. W.; Wade, M. M.; Holman, S. C.; Champlin, F. R. Status of Methods for Assessing Bacterial Cell Surface Charge Properties Based on Zeta Potential Measurements. *J. Microbiol. Methods* **2001**, *43*, 153−164.